Electron-Donating Properties of Boratabenzene Ligands

Guillermo C. Bazan,*,† W. Donald Cotter,‡ Zachary J. A. Komon,† Rip A. Lee,§ and Rene J. Lachicotte§

Contribution from the Department of Chemistry, University of Rochester, Rochester, New York 14627-0216, Department of Chemistry, University of California, Santa Barbara, California 93106, and Mt. Holyoke College, South Hadley, Massachusetts 01075

Received July 9, 1999

Abstract: The reaction of $(C_5H_5B-R)Cp^*ZrMe_2$ ($Cp^* = \eta^5\text{-}C_5Me_5$; R = NMe_2 (**4**), OEt (**5**), Ph (**6**)) with $B(C_6F_5)_3$ affords zwitterionic complexes of the type $[(C_5H_5B-R)Cp^*ZrMe][MeB(C_6F_5)_3]$ (R = NMe_2 (**7**), OEt (**8**), Ph (**9**)). The molecular structures of **7** and **9** were determined by single-crystal X-ray diffraction studies, and they were found to be similar to those observed for standard group 4 metallocenes. The boratabenzene ligand in **7** more closely resembles an η^5-pentadienyl fragment than in **9**, where it is η^6-bound. Variable-temperature ^1H NMR spectroscopy shows that ion-pair dissociation/recombination processes occur in solution. Data over large temperature ranges were obtained by the combination of line shape and spin saturation transfer techniques (100 °C for **4** and **5**, 65 °C for **6**). The rates of these processes give insight into how the orbital overlap between boron and the exocyclic group affects the rates of elementary reactions at the metal. The $\Delta H^\ddagger$ values for ion-pair dissociation/recombination were found to increase with decreasing donor strength of the substituent: 12.2(2), 12.6(1), and 17.6(3) kcal/mol for **7**, **8**, and **9**, respectively. Exchange reactions between **9** and **4** reveal that **7** is formed exclusively, indicating that the aminoboratabenzene ligand can better accommodate the increased positive charge on the metal center. The dependence of the carbonyl stretching frequency on the extent of metal back-bonding in complexes of the type $(C_5H_5B-R)Cp^*Zr(CO)_2$ (R = NMe_2 (**10**), OEt (**11**), Me (**12**), Ph (**13**)) and $(C_5H_5B-R)_2Zr(CO)_2$ (R = NMe_2 (**14**), OEt (**15**), Me (**16**), Ph (**17**)) can also be used to gauge the electron density at Zr. Complexes **10**−**17** were prepared by reductive carbonylation of the corresponding dichlorides. The measured reduction potentials of the dichlorides, $(C_5H_5B-R)_2ZrCl_2$, show that it is progressively more difficult to reduce the metal center as the donor strength of the boratabenzene ligand increases. The dynamic NMR, IR, and electrochemical data are consistent with the notion that the donor properties in $[C_5H_5B-R]$ ligands decrease in the order R = NMe_2 > OEt ≈ Me > Ph.

Introduction

Electron-deficient metallocenes of generic composition [Cp₂MR][NCA] (M= group 4 metal; Cp = η^5-cyclopentadienyl; NCA = noncoordinating anion)[1] are the archetype for the majority of catalysts in homogeneous Ziegler−Natta polymerization.[2] The design and synthesis of these "single-site" catalysts and the study of their structure−reactivity relationships are important themes in catalyst research[3] due to their rising impact in polyolefin technology.[4] Although the literature is replete with innovations in metallocene chemistry, there has been considerable effort in the search for alternative catalysts which contain non-Cp ligand/metal combinations.[5] The aim of these studies is to increase the number of available methods for the prepara-

† University of California.
‡ Mt. Holyoke College.
§ University of Rochester.
(1) (a) Dyachovskii, F. S.; Shilova, A. K.; Shilova, A. E. *J. Polym. Sci., Part C* **1967**, *16*, 2333. (b) Eisch, J. J.; Piotrowski, A. M.; Brownstein, S. K.; Gabe, E. J.; Lee, F. L. *J. Am. Chem. Soc.* **1985**, *107*, 7219. (c) Hlatky, G. G.; Turner, H. W.; Eckman, R. R. *J. Am. Chem. Soc.* **1989**, *111*, 2798. (d) Bochmann, M.; Jaggar, A. J.; Nicholls, J. C. *Angew. Chem., Int. Ed. Engl.* **1990**, *29*, 780. (e) Jordan, R. F. *Adv. Organomet. Chem.* **1991**, *32*, 325. (f) Yang, X.; Stern, C. L.; Marks, T. J. *J. Am. Chem. Soc.* **1991**, *113*, 3623. (g) Bochmann, M. *Angew. Chem., Int. Ed. Engl.* **1992**, *31*, 1181.
(2) (a) *Transition Metals and Organometallics as Catalysts for Olefin Polymerization*; Kaminsky, W., Sinn, H., Eds.; Springer-Verlag: Berlin, 1988. (b) *Ziegler Catalysts*; Fink, G., Mülhaupt, R., Brintzinger, H.-H., Eds.; Springer-Verlag: Berlin, 1995. (c) Kaminsky, W.; Arndt, M. In *Applied Homogeneous Catalysis with Organometallic Compounds*; Cornils, B., Hermann, W. A., Eds.; VCH: Weinheim, Germany, 1995. (d) Tait, P. J. T. In *Polymeric Materials Encyclopedia*; Salamone, J. C., Ed; CRC Press: New York, 1996; Vol. 6, p 4169.

(3) For reviews, see: (a) Mohring, P. C.; Coville, N. *J. Organomet. Chem.* **1994**, *479*, 1. (b) Brintzinger, H. H.; Fischer, D.; Mülhaupt, R.; Rieger, B.; Waymouth, R. M. *Angew. Chem., Int. Ed. Engl.* **1995**, *34*, 1143. (c) Huang, J.; Rempel, G. L. *Prog. Polym. Sci.* **1995**, *20*, 459. (d) Bochmann, M. *J. Chem. Soc., Dalton Trans.* **1996**, 255.
(4) (a) Thayer, A. M. *Chem. Eng. News* **1995** (Sept 11), 15. (b) Montagna, A. A. *CHEMTECH* **1995** (October), 44. (c) Schut, J. H. *Plastics World* **1997** (April), 27. (d) van Arnum, P. *CMR Focus Report* **1998** (April 27) FR 17. (e) Morse, P. M. *Chem. Eng. News* **1998** (Dec 11), 25.
(5) "Hybrid" olefin polymerization precatalysts containing bis(phenoxide),[5a−c] bis(amide),[5d−g] amidinate,[5h−k] bis(quinoxalato),[5l] bis(pyrolyl),[5m] and tridentate ligand sets[5n,o] have been constructed: (a) van der Linden, A.; Schaverien, C. J.; Meijboom, N.; Ganter, C.; Orpen, A. G. *J. Am. Chem. Soc.* **1995**, *117*, 3008. (b) Fokken, S.; Spaniol, T. P.; Okuda, J.; Sernetz, F. G.; Mülhaupt, R. *Organometallics* **1997**, *16*, 4240. (c) Thorn, M. G.; Etheridge, Z. C.; Fanwick, P. E.; Rothwell, I. P. *Organometallics* **1998**, *17*, 3636. (d) Cloke, F. G. N.; Geldbach, T. J.; Hitchcock, P. B.; Love, J. B. *J. Organomet. Chem.* **1995**, *506*, 343. (e) Tinkler, S.; Deeth, R. J.; Duncalf, D. J.; McCamley, A. *Chem. Commun.* **1996**, 2623. (f) Scollard, J. D.; McConville, D. H. *J. Am. Chem. Soc.* **1996**, *118*, 10008. (g) Jeon, Y.-M.; Park, S. J.; Heo, J.; Kim, K. *Organometallics* **1998**, *17*, 3161. (h) Duchateau, R.; Vanwee, C. T.; Meetsma, A.; Teuben, J. H. *J. Am. Chem. Soc.* **1993**, *115*, 4931. (i) Flores, J. C.; Chien, J. C. W.; Rausch, M. D. *Organometallics* **1995**, *14*, 2106. (j) Walther, B.; Fischer, R.; Görls, H.; Koch, J.; Schweder, B. *J. Organomet. Chem.* **1996**, *508*, 13. (k) Averbuj, C.; Tish, E.; Eisen, M. S. *J. Am. Chem. Soc.* **1998**, *120*, 8640. (l) Tsukahara, T.; Swenson, D. C.; Jordan, R. F. *Organometallics* **1997**, *16*, 3303. (m) Etherton, B. P.; Nagy, S. U.S. Patent 5,539,124, 1996. (n) Horton, A. D.; de With, J.; van der Linden, A. J.; van de Weg, H. *Organometallics* **1996**, *15*, 2672. (o) Baumann, R.; Davis, W. M.; Schrock, R. R. *J. Am. Chem. Soc.* **1997**, *119*, 3830.

Table 1. Compound Abbreviation Index

1	$(C_5H_5B-N(i-Pr)_2)ZrCl_2$
2	$(C_5H_5B-OEt)_2ZrCl_2$
3	$(C_5H_5B-Ph)_2ZrCl_2$
4	$(C_5H_5B-NMe_2)Cp*ZrMe_2$
5	$(C_5H_5B-OEt)Cp*ZrMe_2$
6	$(C_5H_5B-Ph)Cp*ZrMe_2$
7	$[(C_5H_5B-NMe_2)Cp*ZrMe][MeB(C_6F_5)_3]$
8	$[(C_5H_5B-OEt)Cp*ZrMe][MeB(C_6F_5)_3]$
9	$[(C_5H_5B-Ph)Cp*ZrMe][MeB(C_6F_5)_3]$
10	$(C_5H_5B-NMe_2)Cp*Zr(CO)_2$
11	$(C_5H_5B-OEt)Cp*Zr(CO)_2$
12	$(C_5H_5B-Me)Cp*Zr(CO)_2$
13	$(C_5H_5B-Ph)Cp*Zr(CO)_2$
14	$(C_5H_5B-NMe_2)_2Zr(CO)_2$
15	$(C_5H_5B-OEt)_2Zr(CO)_2$
16	$(C_5H_5B-Me)_2Zr(CO)_2$
17	$(C_5H_5B-Ph)_2Zr(CO)_2$
18	$(C_5H_5B-NMe_2)_2ZrCl_2$
19	$(C_5H_5B-Me)_2ZrCl_2$

tion of polyolefins with optimized properties and to improve our understanding of how ligand changes affect elementary reaction steps mediated by metal centers.[6]

We recently demonstrated that the boratabenzene[7] fragment is a suitable Cp surrogate and that bis(boratabenzene)zirconium dichlorides, $(C_5H_5B-R)_2ZrCl_2$ (R = N(i-Pr)$_2$ (**1**),[8] OEt (**2**),[9] Ph (**3**)[10]), are capable of sustaining high levels of catalysis when activated with methylaluminoxane (MAO). (Table 1 contains the numbering scheme for all compounds in this paper.)

1, R = N(*i*-Pr)$_2$
2, R = OEt
3, R = Ph
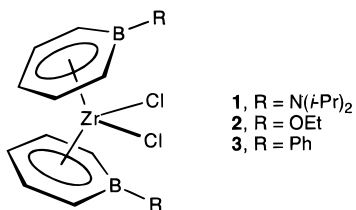
Importantly, we have shown that the exocyclic substituent on boron controls the type of product formed. When 1 atm of ethylene is used, **1**/MAO/C_2H_4 gives polyethylene while **3**/MAO/C_2H_4 affords primarily 2-alkyl-1-alkenes. Furthermore, one obtains 1-alkenes exclusively using **2**/MAO/C_2H_4. From these observations, and from the structural characterization of the *precatalysts* **1**–**3**, we proposed that the extent of π-donation of the substituent alters the zirconium–boron orbital overlap and, ultimately, the reactivity of the metal.[11] Aromatic delocalization within the aminoboratabenzene framework is attenuated by the interaction of the nitrogen lone pair with boron.[12] As a result, the aminoboratabenzene ligand in **1** is pentadienyl-like and

coordinates to zirconium in an η^5-fashion.[8] When the π-interaction is weaker, as in **3**, the boratabenzene is best described as an η^6-bound, aromatic ligand.[9,10] Consequently, the metal center in **1** is expected to be less electrophilic than in **3**.

In this contribution, we first evaluate the electronic influence of the exocyclic substituent on the rates of elementary reactions in *zwitterionic* complexes of the type, $[(C_5H_5B-R)Cp*ZrMe]$-$[MeB(C_6F_5)_3]$ (Cp* = η^5-C_5Me_5; R = NMe$_2$ (**7**), OEt (**8**), Ph (**9**)), which more closely resemble the putative catalysts in the MAO reactions.[1] The isolation and characterization of **7**–**9** confirms that the use of boratabenzene ligands as a Cp substitute leads to well-defined catalysts of similar structure. In an effort to correlate reactivity with ligand donor properties, we examined two parameters that should be sensitive to the electron density at the metal. For a spectroscopic signature, we synthesized zirconium dicarbonyl compounds with different boratabenzene environments and measured the carbonyl stretching frequencies. Furthermore, the reduction potentials of the bis(boratabenzene)-zirconium dichlorides were also examined. These measurements form a base from which we may correlate the electronic characteristics at zirconium with an easily identifiable reaction profile. Ultimately, this information should allow us to extend this class of catalysts to other catalytic reactions[11] or to applications in organic transformations.[13]

Results and Discussion

The preparation of boratabenzene-containing, dimethylzirconium complexes from their dichlorides is not straightforward. Alkylation with MeMgBr or MeLi is complicated by boron's susceptibility to nucleophilic attack,[14] which results in low reaction yields and in the formation of side products which are difficult to separate. Repeated attempts to obtain preparative-scale quantities of analytically pure $(C_5H_5B-R)_2ZrMe_2$ in high yields have met with little success.[15] In view of these difficulties, the current synthetic strategy relies on alkylation of the metal *prior to* boratabenzene coordination.[16] We also anticipated that a combination with the Cp* ligand would lead to more crystalline and more stable compounds. Thus, the dimethyl precursors, $(C_5H_5B-R)Cp*ZrMe_2$ (R = NMe$_2$ (**4**), OEt (**5**), Ph (**6**)), were prepared by metathetical reactions of the appropriate alkali boratabenzene salt with Cp*ZrMe$_2$Cl (eq 1).

Cp*ZrMe$_2$Cl

+

M(C$_5$H$_5$B-R)

M = Li, Na

4, R = NMe$_2$
5, R = OEt
6, R = Ph

(1)
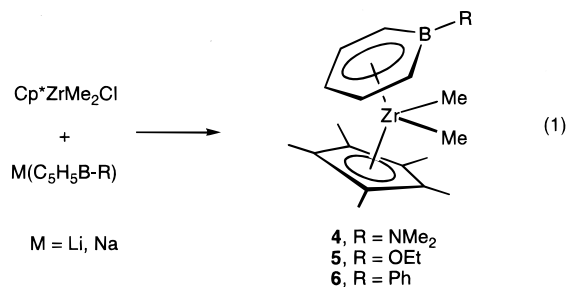
The reactions in eq 1 proceed in excellent yields by ^{1}H NMR spectroscopy; however, these yellow complexes may be isolated only in modest yields owing to their extreme solubility in

(6) (a) Margl, P.; Deng, L.; Ziegler, T. *Organometallics* **1998**, *17*, 933. (b) Margl, P.; Deng, L.; Ziegler, T. *J. Am. Chem. Soc.* **1998**, *120*, 5517.

(7) Herberich, G. E.; Greiss, G.; Heil, H. F. *Angew. Chem., Int. Ed. Engl.* **1970**, *9*, 805. (b) Ashe, A. J., III; Shu, P. *J. Am. Chem. Soc.* **1971**, *93*, 1804. (c) Sullivan, S. A.; Sandford, H.; Beauchamp, J. L.; Ashe, A. J., III *J. Am. Chem. Soc.* **1978**, *100*, 3737. (d) Herberich, G. E.; Ohst, H. *Adv. Organomet. Chem.* **1986**, *25*, 199. (e) Herberich, G. E.; Schmidt, B.; Englert, U. *Organometallics* **1995**, *14*, 471. (f) Hoic, D. A.; Wolf, J. R.; Davis, W. M.; Fu, G. C. *Organometallics* **1996**, *15*, 1315. (g) Qiao, S.; Hoic, D. A.; Fu, G. C. *J. Am. Chem. Soc.* **1996**, *118*, 6329.

(8) Bazan, G. C.; Rodriguez, G.; Ashe, A. J., III; Al-Ahmad, S.; Müller, C. *J. Am. Chem. Soc.* **1996**, *118*, 2291.

(9) Rogers, J. S.; Bazan, G. C.; Sperry, C. K. *J. Am. Chem. Soc.* **1997**, *119*, 9305.

(10) Bazan, G. C.; Rodriguez, G.; Ashe, A. J., III; Al-Ahmad, S.; Kampf, J. W. *Organometallics* **1997**, *16*, 2492.

(11) Bönnemann, H. *Angew. Chem., Int. Ed. Engl.* **1985**, *24*, 248.

(12) (a) Herberich, G. E.; Schmidt, B.; Englert, U.; Wagner, T. *Organometallics* **1993**, *12*, 2891. (b) Ashe, A. J., III; Kampf, J. W.; Müller, C.; Schneider, M. *Organometallics* **1996**, *15*, 387.

(13) Shaughnessy, K. H.; Waymouth, R. M. *Organometallics* **1998**, *17*, 5728.

(14) This problem has been noted previously and has been documented to be a function of the boron substituent. See refs 8 and 10.

(15) Attempts to prepare $(C_5H_5B-R)_2ZrMe_2$ using "ZrMe$_2$Cl$_2$" were not successful, presumably due to the highly reducing reaction conditions. See: Park, J. T.; Woo, B. W.; Yoon, S. C.; Shim, S. C. *J. Organomet. Chem.* **1997**, *535*, 29.

(16) Lee, R. A.; Lachicotte, R. J.; Bazan, G. C. *J. Am. Chem. Soc.* **1998**, *120*, 6037.

common organic solvents. Despite the overall loss in yields, recrystallization is recommended for success in subsequent reactions.

The zwitterionic compounds **7**, **8**, and **9** were synthesized by the slow addition of the methide-abstracting reagent, $B(C_6F_5)_3$,[17] with **4**, **5**, and **6**, respectively (eq 2).[18] These reactions are rapid
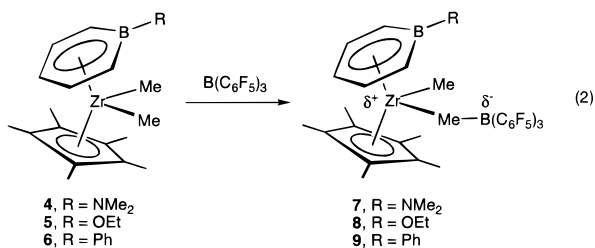
and proceed quantitatively, as revealed by ^1H NMR spectroscopy. Complexes **7**−**9** are stable in toluene at room temperature for up to 1 week; they form oils in benzene, and they decompose instantly in CH_2Cl_2. They may be isolated by precipitation with pentane. Deep red crystals of **7** form when concentrated solutions are stored for prolonged periods at low temperature. In contrast, yellow microcrystals of **9** precipitate out of concentrated toluene solutions at room temperature within minutes. Compound **8** could only be isolated as a yellow powder.

The crystallographically determined geometry of **7** is similar to the structures determined by Marks and co-workers for metallocene counterparts.[19] Compound **7** consists of an ion pair containing a [(C_5H_5B−NMe_2)Cp*ZrMe] cation and a [MeB-$(C_6F_5)_3$] anion (Figure 1). The two partners are connected via an asymmetric Zr···H_3C−B bridge. The methyl group of the anion is directed toward the cleft of the metallocene with a Zr(1)−C(2) bond length and Zr(1)···C(1) distance (2.281(4) and 2.550(4) Å, respectively) comparable to those observed in [Cp″$_2$ZrMe][MeB($C_6F_5)_3$] (Cp″ = η^5-1,2-Me$_2C_5H_3$) (2.252(4) and 2.549(3) Å).[1f,20a] The hydrogen atoms were located, and there is one close contact to zirconium with a Zr(1)···H(1) distance of 2.22(4) Å while the other two are slightly farther apart (2.41(4) and 2.60(4) Å). Coordination of the boron-bound methyl group to the metal by Zr−H interactions of this type has been observed previously.[21] The aminoboratabenzene ligand is η^5-pentadienyl-like, as shown by the approximately 11° puckering of the boron atom out of the plane defined by the five ring carbon atoms and by the long Zr(1)···B(1) distance (2.899(4) Å).

The molecular structure of **9** (Figure 2) is similar in many ways to that of **7** (i.e., Zr(1)−C(2) = 2.265(2) Å and Zr(1)···C(2) = 2.547(2) Å). However, within the [(C_5H_5B−Ph)Cp*ZrMe] fragment, there is an η^6-bound phenylboratabenzene
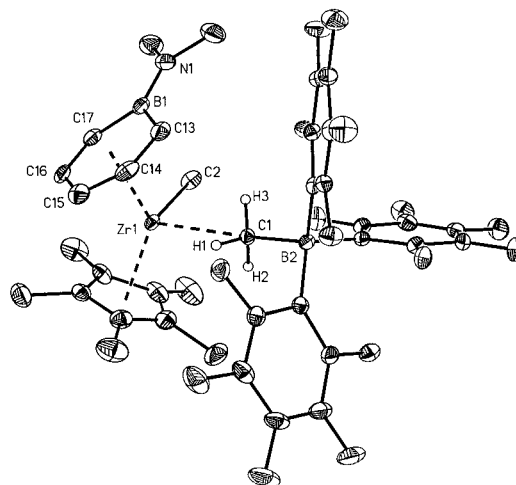
Figure 1. ORTEP view of **7**. Thermal ellipsoids are shown at the 30% probability level. Selected interatomic distances (Å): Zr(1)···C(1) = 2.551(4), Zr(1)−C(2) = 2.281(4), Zr(1)−B(1) = 2.889(4), B(1)−N(1) = 1.396(7), B(2)−C(1) = 1.664(6).
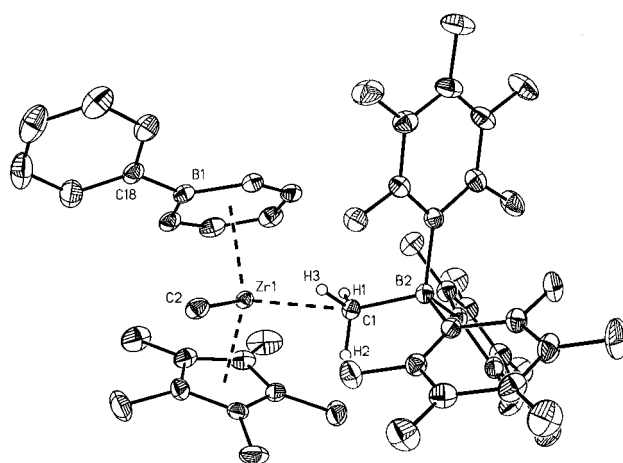
Figure 2. ORTEP view of **9**. Thermal ellipsoids are shown at the 30% probability level. Selected interatomic distances (Å): Zr(1)···C(1) = 2.548(2), Zr(1)−C(2) = 2.265(2), Zr(1)−B(1) = 2.770(2), B(1)−C(18) = 1.562(3), B(2)−C(1) = 1.667(3).

zene ligand in which the pendant phenyl group is nearly coplanar with the heterocyclic ring (Zr(1)···B(1) distance = 2.770(2) Å).

The structural features in the incipient cations follow the trends observed in the precatalysts **1** and **3**, namely, the increase in the Zr−B distance with strong π-donor substituents is maintained. Apart from this distortion, the metrical measurements in **7** and **9**, specifically the cation−anion separation, are statistically identical. Thus, any differences in the extent of Coulombic attraction between ions, which could indicate a reactivity difference, are not detected.

Solution Dynamics of 7−9. The solution dynamics of metallocenium ion pairs such as [Cp″$_2$ZrMe][MeB($C_6F_5)_3$] have

(17) (a) Massey, A. G.; Park, A. J. *J. Organomet. Chem.* **1964**, *2*, 245. (b) Massey, A. G.; Park, A. J. *J. Organomet. Chem.* **1966**, *5*, 218.

(18) For other examples of the role of B($C_6F_5)_3$ in alkyl abstraction, see: (a) Yang, X.; Stern, C. L.; Marks, T. J. *J. Am. Chem. Soc.* **1991**, *113*, 3623. (b) Quyoum, R.; Wang, Q.; Tudoret, M.-J.; Baird, M. C.; Gillis, D. J. *J. Am. Chem. Soc.* **1994**, *116*, 6435. (c) Pellecchia, C.; Pappalardo, D.; Oliva, L.; Zambelli, A. *J. Am. Chem. Soc.* **1995**, *117*, 6593. (d) Wu, Z.; Jordan, R. F. *J. Am. Chem. Soc.* **1995**, *117*, 5867. (e) Horton, A. D. *Organometallics* **1996**, *15*, 2675. (f) Scollard, J. D.; McConville, D. H.; Rettig, S. J. *Organometallics* **1997**, *16* 1810. (g) Witte, P.; Meetsma, A.; Hessen, B. *J. Am. Chem. Soc.* **1997**, *119*, 10561. (h) van der Heijden, H.; Hessen, B.; Orpen, A. G. *J. Am. Chem. Soc.* **1998**, *120*, 1112.

(19) (a) Yang, X.; Stern, C. L.; Marks, T. J. *J. Am. Chem. Soc.* **1994**, *116*, 10015. (b) Bochmann, M.; Lancaster, S. J.; Hursthouse, M. B.; Abdul Malik, K. M. *Organometallics* **1994**, *13*, 2235.

(20) (a) Deck, P. A.; Marks, T. J. *J. Am. Chem. Soc.* **1995**, *117*, 6128. (b) Deck, P. A.; Beswick, C. L.; Marks, T. J. *J. Am. Chem. Soc.* **1998**, *120*, 1772.

(21) Recent studies show that the extent of ion pairing is intimately connected to the nature of the counteranion. See: (a) Eisch, J. J.; Pombrik, S. I.; Zheng, G.-X. *Organometallics* **1993**, *12*, 3856. (b) Siedle, A. R.; Lamanna, W. M.; Newmark, R. A. *Makromol. Chem., Macromol. Symp.* **1993**, *66*, 215. (c) Vizzini, J. C.; Chien, J. C. W.; Babu, G. N.; Newmark, R. A. *J. Polym. Sci., Part A: Polym. Chem.* **1994**, *32*, 2049. (d) Chien, J. C. W.; Song, W.; Rausch, M. D. *J. Polym. Sci., Part A: Polym. Chem.* **1994**, *32*, 2387. (e) Jia, L.; Yang, X.; Ishihara, A.; Marks, T. J. *Organometallics* **1995**, *14*, 3135. (f) Chen, Y.-X.; Stern, C. L.; Yang, S.; Marks, T. J. *J. Am. Chem. Soc.* **1996**, *118*, 12451. (g) Jia, L.; Yang, X.; Stern, C. L.; Marks, T. J. *Organometallics* **1997**, *16*, 842. (h) Tritto, I.; Donetti, R.; Sacchi, M. C.; Locatelli, P.; Zannoni, G. *Macromolecules* **1997**, *30*, 1247.

been elucidated in an elegant series of reports by Marks and co-workers.[20] Dynamic NMR studies delineate two exchange processes: (1) ion-pair dissociation/recombination, involving site exchange of the Zr-bound methyl group and the [MeB-$(C_6F_5)_3$] anion within the equatorial plane of the metallocene (eq 3), and (2) Zr−Me/B−Me exchange, which requires the dissociation of $B(C_6F_5)_3$ followed by recombination.

$$\text{(3)}$$
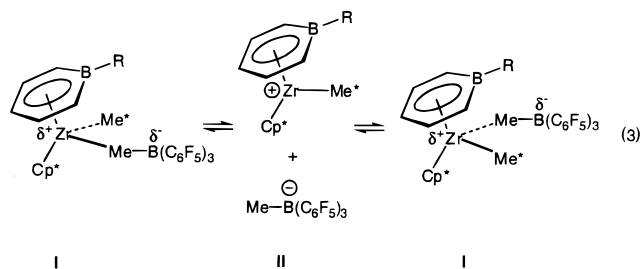
We reasoned that solution dynamics studies might provide an incisive probe for assessing boron substituent effects. In particular, a comparison of the activation parameters for the ion-pair dissociation/recombination process would lend insight into the relative strengths of ion pairing in **7**−**9**. Ion-pair separation is a necessary step for olefin insertion, and it is directly related, inter alia, to the localization of charge on the metal.[21] As **7**−**9** are active, single-component ethylene polymerization catalysts,[22] measuring their exchange rates is relevant to understanding how boratabenzene ligands affect elementary steps in catalysis.

The ^{1}H NMR spectra (in toluene-d_8) of **7** at 228 K, **8** at 243 K, and **9** at 258 K exhibit five separate resonances for each of the boratabenzene ring hydrogens. Coalescence of the two sets of H_α and H_β (relative to boron) signals is observed upon raising the temperature until only three resonances are observed at the high-temperature limit. The single H_γ resonance is unaffected, and the process is reversible (Figure 3). The two methyl resonances remain inequivalent throughout the dynamic event. These observations are consistent with an ion-pair dissociation/recombination process, in which enantiomeric structures corresponding to **I** are interconverted via the caged, or solvent-separated, species **II** (see eq 3).[21]

The rate constants as a function of temperature for **7**−**9** were obtained by line shape analyses of the variable-temperature NMR spectra using the program DNMR 5.[23,24] These rate constants were found to be independent of concentration. We should note here that [(C$_5$H$_5$B−*Me*)Cp*ZrMe][MeB(C$_6$F$_5$)$_3$] is easily prepared from the known (C$_5$H$_5$B−Me)Cp*ZrMe$_2$.[45] However, the rates of exchange measured for [(C$_5$H$_5$B−Me)-Cp*ZrMe][MeB(C$_6$F$_5$)$_3$] proved to be concentration dependent and will not be considered in further discussion.

The activation parameters for **7**−**9** were obtained from least-squares analyses of the Eyring plots. Rate constants over a reasonably wide (60 deg) temperature range were measured for compounds **7** and **8**. However, line shape analysis for the phenylboratabenzene complex, **9**, was limited to a narrower temperature range (25 deg) due to the greater temperature

(22) Ethylene polymerization activities for **7**, **8**, and **9** ([Zr] = 1.5 × 10^{-4} M, 1 atm, 23 °C) are 323, 276, and 290 kg PE/mol of Zr/h, respectively. Polymerization procedures can be found in ref 16 and in the following: Rogers, J. S.; Lachicotte, R. J.; Bazan, G. C., *J. Am. Chem. Soc.* **1999**, *121*, 1288.

(23) Sandstrøm, J. *Dynamic NMR Spectroscopy*; Academic Press: New York, 1982.

(24) Stephenson, D. S.; Binsch, G.; LeMaster, C. L.; True, N. S. *Program QCMP059*; Quantum Chemistry Program Exchange; Indiana University: Bloomington, IN.
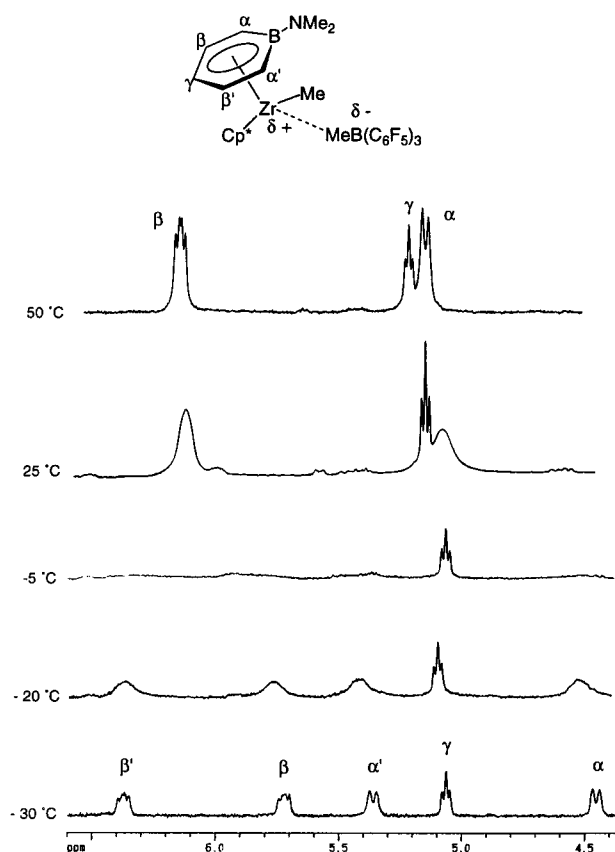
Figure 3. Variable-tempterature ^{1}H NMR spectra (toluene-d_8) of **7** in the aromatic region.

dependence of the observable dynamic event. Since narrow temperature ranges do not allow for accurate $\Delta H^{\ddagger}$ and $\Delta S^{\ddagger}$ determinations,[25] we focused on spin saturation transfer experiments[26] to extend the temperature range of the rate data.

The method described originally by Forsén and Hoffman was used.[26a] In our case, one of the H_α (or H_β) signals was irradiated selectively using a 90° pulse, and a decrease in the intensity of the exchanging H_α' (or H_β') resonance was observed. Under steady-state conditions, the rate constant can be calculated according to the equation

$$k = \frac{1}{T_1}\left(\frac{I_0}{I} - 1\right)$$

where T_1 is the spin−lattice relaxation time; I and I_0 are the intensities of the H_α' (or H_β') resonance with and without saturation of the H_α (or H_β) resonance, respectively.[26e,h] The H_γ and Cp* resonances served as internal standards.

Figure 4 shows the Eyring plots for ion-pair dissociation/recombination for compounds **7**−**9**. The data points which were

(25) Steigel, A.; Sauer, J.; Kleier, D. A.; Binsch, G. *J. Am. Chem. Soc.* **1972**, *94*, 2770.

(26) For discussion, see: (a) Forsén, S.; Hoffman, R. A. *J. Chem. Phys.* **1963**, *39*, 2892. (b) Anet, F. A. L.; Bourn, A. J. R. *J. Am. Chem. Soc.* **1967**, *89*, 760. (c) Baine, P.; Gerig, J. T.; Stock, A. D. *J. Magn. Reson.* **1981**, *17*, 41. (d) Freeman, R. *A Handbook of Nuclear Magnetic Resonance Spectroscopy*; Longman Scientific & Technical: Essex, 1988. (e) Jarek, R. L.; Flesher, R. J.; Shin, S. K. *J. Chem. Educ.* **1997**, *74*, 1. For applications in organometallic systems, see: (f) Doherty, N. M.; Bercaw, J. E. *J. Am. Chem. Soc.* **1985**, *107*, 2670. (g) Wang, Q.; Gillis, D. J.; Quyoum, R.; Jeremic, D.; Tudoret, M.-J.; Baird, M. C. *J. Organomet. Chem.* **1997**, *527*, 7. (h) Amor, J. I.; Cuenca, T.; Galakhov, M.; Gomez-Sal, P.; Manzanero, A.; Royo, P. *J. Organomet. Chem.* **1997**, *535*, 155. (i) Sola, E.; Bakhmutov, V. I.; Torres, F.; Elduque, A.; Lopez, J. A.; Lahoz, F. J.; Werner, H.; Oro, L. A. *Organometallics* **1998**, *17*, 683.
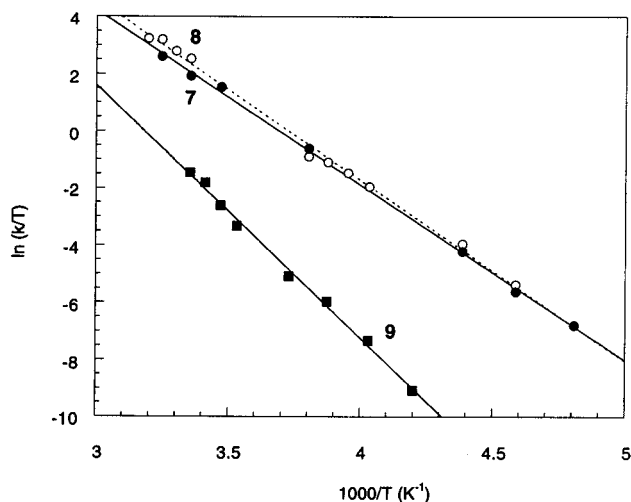
Figure 4. Eyring plot for ion-pair dissociation/recombination for **7**–**9**.

Table 2. Activation Parameters for Ion-Pair Dissociation/Recombination Processes of [(C₅H₅B−R)Cp*ZrMe][MeB(C₆F₅)₃] in Toluene-d_8

R	$\Delta H^{\ddagger}$ (kcal/mol)	$\Delta S^{\ddagger}$ (eu)	$\Delta G^{\ddagger}$ 298(kcal/mol)
NMe₂ (**7**)	12.2(2)	−2.3(6)	12.9(6)
OEt (**8**)	12.6(1)	−0.5(4)	12.7(4)
Ph (**9**)	17.6(3)	8(1)	15(1)

obtained by the combination of the two experimental techniques and which span a 100-deg temperature range for **7** and **8** (65-deg range for **9**) match well. Activation parameters derived from these plots are listed in Table 2. Experimental errors for these activation parameters were calculated from error propagation formulas derived from the Eyring equation as shown by Girolami.[27]

The $\Delta H^{\ddagger}$ values are considerably different for the complexes with π-donor substituents, **7** and **8** (12.2(2) and 12.6(1) kcal/mol, respectively), relative to **9** (17.6(3) kcal/mol). The slight difference between $\Delta H^{\ddagger}$ terms **7** and **8** may reflect the greater donor strength of the dimethylamino substituent vis-à-vis ethoxy.[9,12,28] For **9**, the unfavorable activation enthalpy is partially compensated by a gain in entropy, most simply interpreted as the creation of two largely independent, ionic particles from one closely associated pair. Ion-pair dissociation in **7** and **8** is close to entropically neutral, suggesting a lesser change in the degrees of freedom between structures **I** and **II**, and thus a more electronically saturated zirconium center. Additional solvent−dipole organization in the transition state may contribute to the small, negative $\Delta S^{\ddagger}$ observed for complex **7**.

The strength of ion-pairing in these compounds is also evident in the ¹H NMR spectra at their slow-exchange limits. The significantly larger chemical shift difference between the two diastereotopic H$_\alpha$ resonances in **9** ($\Delta\delta$ = 1.6 ppm compared to 0.9 ppm for **7** and **8**) indicates a greater disparity between the chemical environments of the two sides of these boratabenzene rings. It follows that, on average, the anion is held more tightly to the zirconium core in **9** than it is in either **7** or **8**.[29]

Ground-State Preferences. While the exchange reactions described in the preceding section correspond to the activation energies for a given substituent, it would be of interest to explore the relative aptitudes of different [C₅H₅B−R] ligands in accommodating the reduced electron density at the metal center. To accomplish a relative comparison, we explored the possibility of exchange reactions involving zwitterionic [(C₅H₅B−R₁)Cp*ZrMe][MeB(C₆F₅)₃] and neutral (C₅H₅B−R₂)-Cp*ZrMe₂ complexes with different R₁ and R₂ groups as illustrated in eq 4. Ideally, one would like to measure the value of the equilibrium constant, *K*, in eq 4 for a series of pairs, R₁ and R₂.

(4)
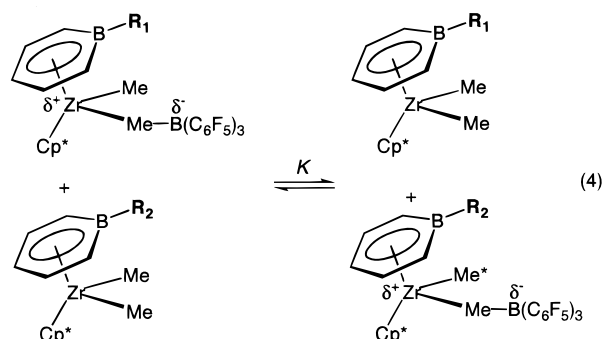
The principal obstacle in these experiments is the formation of oily products. When 1 equiv each of **4** and **9** are mixed in toluene, the product phase separates from solution and cannot be characterized by ¹H NMR spectroscopy. We suspect that bridging species such as the one shown below are formed.[30]
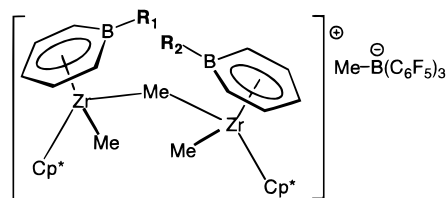
In THF-d_8, the spectroscopic data for **7**–**9** are consistent with cleavage of the ion pair and coordination of THF-d_8, resulting in the formation of [(C₅H₅B−R)Cp*ZrMe(THF-d_8)][MeB-(C₆F₅)₃]. No reactions occur when combinations of solutions of **4**–**6** and **7**–**9** in THF-d_8 are mixed, even after heating at 60 °C for 1 week. Therefore, THF is sufficiently polar to solubilize the charged species and binds strongly to zirconium to prevent disproportionation reactions.[31] A final set of experiments involved the addition of **4** to **9** in toluene-d_8 and dissolving the resulting oil in THF-d_8. Only **7**·THF-d_8 and (C₅H₅B−Ph)-Cp*ZrMe₂ (**6**) were observed. A similar reaction was performed starting with **7** and **6**, and ¹H NMR analysis of the redissolved oil showed that **7**·THF-d_8 and **6** were formed. The same products were observed when 1 equiv of B(C₆F₅)₃ was added to an equimolar mixture of **4** and **6**. In all three cases, **7**·THF-d_8 is the only cationic species formed (eq 5). These experiments demonstrate that (dimethylamino)boratabenzene lowers the

(27) Morse, P. M.; Spencer, M. D.; Wilson, S. R.; Girolami, G. S. *Organometallics* **1994**, *13*, 1646.

(28) (a) *The Chemistry of Boron and Its Compounds*; Muetterties, E. L., Ed.; John Wiley & Sons: New York, 1967. (b) Greenwood, N. N. In *Comprehensive Inorganic Chemistry*; Bailar, J. C., Jr., Eméléus, H. J., Nyholm, R., Trotman-Dickenson, A. F., Eds.; Pergamon Press: Oxford, 1973; Vol. 1, p 665.

(29) The $\Delta(m,p$-F) (¹⁹F NMR) values for compounds **7**–**9** are in the 4.8−5.2 ppm range, which are consistent with a coordinated [MeB(C₆F₅₃] anion. See ref 5n.

(30) For dinuclear cationic intermediates, see: Bochmann, M.; Lancaster, S. J. *Angew. Chem., Int. Ed. Engl.* **1994**, *33*, 1634.

(31) For representative work using Cp₂ZrR(THF)⁺ complexes, see: (a) Jordan, R. F.; Bajgur, C. S.; Willett, R.; Scott, B. *J. Am. Chem. Soc.* **1985**, *107*, 2670. (b) Jordan, R. F.; LaPointe, R. E.; Bradley, P. K.; Baenziger, N. *Organometallics* **1989**, *8*, 2892. (c) Jordan, R. F.; Bradley, P. K.; Baenziger, N. C.; LaPointe, R. E. *J. Am. Chem. Soc.* **1990**, *112*, 1289.

energy of the zwitterionic species relative to phenylboratabenzene, by more readily accommodating the partial positive charge on Zr.
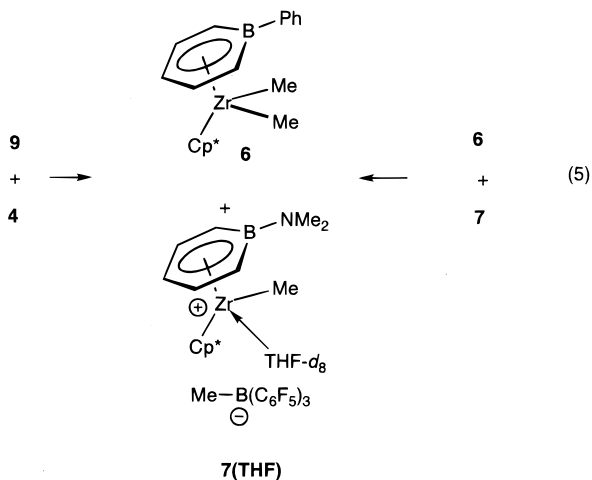
IR and Electrochemical Characterization. To establish an independent probe for the electron density at the metal as a function of the boron substituent, we capitalized on the fact that the carbonyl stretching frequencies in metal carbonyl complexes are sensitive to the degree of back-bonding.[32] Thus, the set of dicarbonyl complexes $(C_5H_5B-R)Cp^*Zr(CO)_2$ (R = NMe_2 (**10**), OEt (**11**), Me (**12**), Ph (**13**)) were prepared by reductive carbonylation of their corresponding dichlorides in the presence of excess Mg in THF (eq 6).
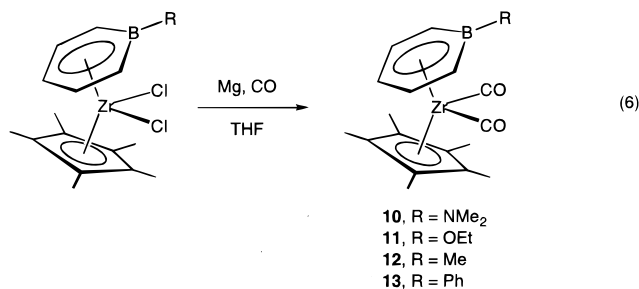
The series of complexes $(C_5H_5B-R)_2Zr(CO)_2$ (R = NMe_2 (**14**), OEt (**15**), Me (**16**), Ph (**17**)) were prepared in a similar manner (eq 7).
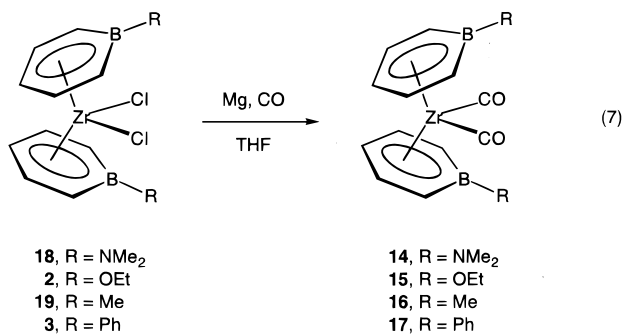
Two $\nu(CO)$ bands, corresponding to the asymmetric and symmetric stretching combinations, are observed for compounds **10**–**17** (Table 3).[33] Lower stretching frequencies indicate

(32) Lukehart, C. M. *Fundamental Transition Metal Organometallic Chemistry*; Brooks/Cole: Monterey, 1985.
(33) Sikora, D. J.; Macomber, D. W.; Rausch, M. D. *Adv. Organomet. Chem.* **1986**, *25*, 317.

Table 3. Carbonyl Stretching Frequencies

compound	$\nu(CO)$ $(cm^{-1})^a$
$(C_5H_5B-NMe_2)Cp^*Zr(CO)_2$ (**10**)	1976, 1908
$(C_5H_5B-Me)Cp^*Zr(CO)_2$ (**12**)	1981, 1913
$(C_5H_5B-OEt)Cp^*Zr(CO)_2$ (**11**)	1982, 1914
$(C_5H_5B-Ph)Cp^*Zr(CO)_2$ (**13**)	1987, 1920
$(C_5H_5B-NMe_2)_2Zr(CO)_2$ (**14**)	2005, 1955
$(C_5H_5B-Me)_2Zr(CO)_2$ (**16**)	2012, 1964
$(C_5H_5B-OEt)_2Zr(CO)_2$ (**15**)	2017, 1969
$(C_5H_5B-Ph)_2Zr(CO)_2$ (**17**)	2018, 1966
$Cp^*_2Zr(CO)_2$	$1945, 1852^b$
$Cp^*CpZr(CO)_2$	$1965, 1875^c$
$Cp_2Zr(CO)_2$	$1975, 1885^b$

^{a} In Nujol. ^{b} In hexane, ref 47. ^{c} In pentane, ref 47.
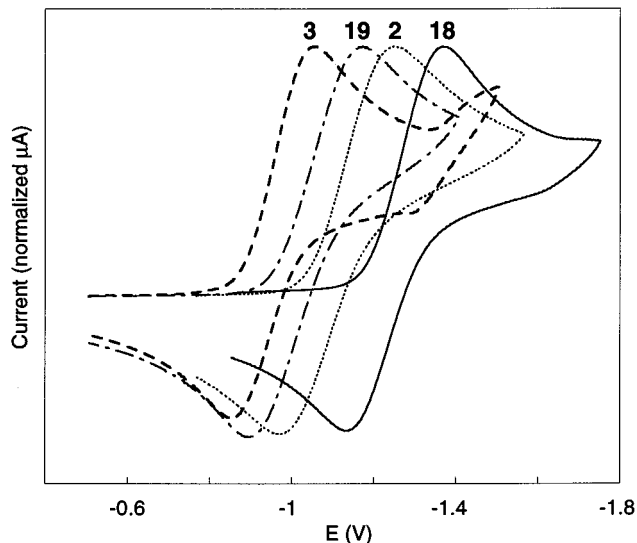
Figure 5. Normalized cyclic voltammograms for **2**, **3**, **18**, and **19** (0.001 M, 0.1 M Bu_4NPF_6, 200 mV/s) in THF. Referenced against SCE.

increased electron density at the metal. Although the range of $\nu(CO)$s is limited,[34] these data show that, for the mixed-ring compounds, substituent donor properties follow the order NMe_2 > OEt ≈ Me > Ph. For the bis(boratabenzene)$Zr(CO)_2$ series the observed ranking is NMe_2 > Me > OEt ≈ Ph. Significantly larger differences in $\nu(CO)$s are observed with Cp^*/Cp/ boratabenzene substitution.

Electrochemical studies have been used to gauge directly the relative amount of electron density at the metal in standard metallocenes.[35] The reduction potentials of the series $(C_5H_5B-R)_2ZrCl_2$ (R = OEt (**2**), Ph (**3**), NMe_2 (**18**), Me (**19**)) were measured by cyclic voltammetry (Figure 5). Each compound exhibits a reversible, one-electron reduction (referenced to ferrocene). The reduction potentials of **2**, **3**, **18**, **19**, and Cp_2ZrCl_2 are listed in Table 4. Increased negative values correspond to metal centers that are more difficult to reduce and thus that are more electron rich. These considerations would order the donor strength of the $[C_5H_5B-R]$ ligands as NMe_2 > OEt > Me > Ph. The reduction potentials for the mixed-ring compounds, $(C_5H_5B-R)Cp^*ZrCl_2$, lie beyond the range of

(34) Comparable shifts in $\nu(CO)$ reflect environment changes brought about by ansa annelation; see: Lee, H.; Desrosiers, P. J.; Guzei, I.; Rheingold, A. L.; Parkin, G. *J. Am. Chem. Soc.* **1998**, *120*, 3255.
(35) (a) Holloway, J. D. L.; Geiger, W. E., Jr. *J. Am. Chem. Soc.* **1979**, *101*, 2038. (b) Lappert, M. F.; Pickett, C. J.; Riley, P. I.; Yarrow, P. I. W. *J. Chem. Soc., Dalton Trans.* **1981**, 805. (c) Finke, R. G.; Gaughan, G.; Voegeli, R. *J. Organomet. Chem.* **1982**, *229*, 179. (d) Gassman, P. G.; Macomber, D. W.; Hershberger, J. W. *Organometallics* **1983**, *2*, 1471. (e) Bajgur, C. S.; Tikkanen, W. R.; Petersen, J. L. *Inorg. Chem.* **1985**, *24*, 2539.

Table 4. Reduction Potentials for $(C_5H_5B-R)_2ZrCl_2$ Complexes vs SCE

R	$E°$ (V)[a]
NMe$_2$ (**18**)	−1.252
OEt (**2**)	−1.110
Me (**19**)	−1.034
Ph (**3**)	−0.954
Cp$_2$ZrCl$_2$[b]	−1.70[b]

[a] Potentials were measured in THF with the use of internally referenced Cp_2Fe^+/Cp_2Fe couple, $E° = 0.51$ V vs SCE, as the internal standard. [b] Listed for comparison.

Table 5. Crystal and Structure Refinement Data for **7** and **9**

cryst params	7	9
chemical formula	$C_{40.5}H_{36}B_2F_{15}NZr$	$C_{48}H_{39}B_2F_{15}Zr$
fw	934.54	1013.63
crystal syst	monoclinic	monoclinic
space group (No.)	$P2_1/c$ (14)	$P2_1/c$ (14)
color of cryst	red	yellow
Z	4	4
a, Å[a]	9.26450(10)	12.3021(2)
b, Å	20.1918(2)	17.4791(2)
c, Å	20.73320(10)	19.6184(3)
α, deg	90	90
β, deg	91.12	93.0690(10)
γ, deg	90	90
vol, Å^3	3877.75(6)	4212.49
d (calc), g/cm^3	1.601	1.598
temp, K	193(2)	193(2)
total no. of reflns	22182	24782
no. of obsd data[c]	6539	8274
no. varied	537	595
R1(F_o), wR2(F_o^2) %[b,c]	6.64, 14.42	3.96, 9.00
goodness-of-fit on F^2 [d]	1.067	1.034

[a] It has been noted that the integration program SAINT produces cell constant errors that are unreasonably small, since systematic error is not included. More reasonable errors might be estimated at 10× the listed values. [b] $R_{int} = \sum|F_o^2 - F_o^2(\text{mean})|/\sum[F_o^2]$. [c] R1 = $(\sum||F_o| - |F_c||)/\sum|F_o|$, wR2 = $[\sum[w(F_o^2 - F_c^2)^2]/\sum[w(F_o^2)^2]]^{1/2}$, where $w = 1/[\sigma^2(F_o) + (aP)^2 + bP]$ and $P = [(\text{Max};0, F_o^2) + 2F_c^2]/3$. [c] GOF = $[\sum[w(F_o^2 - F_c^2)^2]/(n-p)]^{1/2}$, where n and p denote the number of data and parameters.

detection (-3.0 V), further emphasizing the stronger π-basicity of Cp* compared to boratabenzene.

Correlation of Substituent Effects. It is interesting that the electron-donating properties of [C_5H_5B-OEt], in which the exocyclic oxygen atom is capable of π orbital overlap with boron, are similar to those of [C_5H_5B-Me]. From the stretching frequencies of the dicarbonyl complexes we find that [C_5H_5B-Me] appears to be the stronger donor, while the electrochemical data suggest that [C_5H_5B-OEt] is stronger. A well-established method for correlating changes in the reactivity of an organic aromatic compound against the properties of ring substituents makes use of the Hammett equation.[36] Although this linear free energy relationship is typically used to describe the relative reactivities of substrates, the analysis can be extended to various physical measurements. For example, the correlation of intramolecular electronic interactions in substituted ferrocenes with their reduction potentials has been studied extensively.[37] In the preceding sections, we have put forth evidence to show that boron substituent effects are manifested in electrochemical and
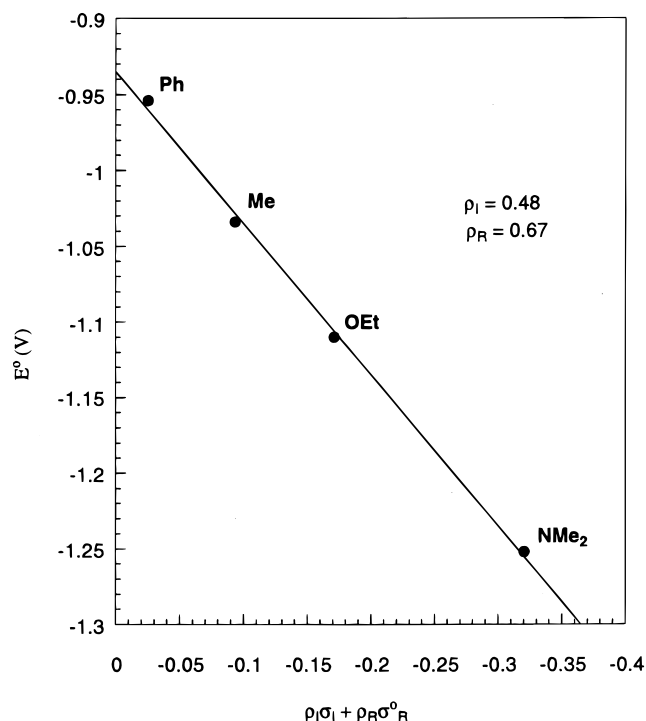
Figure 6. Hammett plot of reduction potentials of $(C_5H_5B-R)_2ZrCl_2$ vs $\rho_I\sigma_I + \rho_R\sigma°_R$.

spectroscopic measurements of a set of related compounds. Since boratabenzenes are isostructural with and isoelectronic to benzene, we reasoned that a Hammett analysis could be useful in ascertaining whether the transmission of electronic effects in boratabenzenes is similar to that observed in the well-understood, substituted aromatic systems.

The standard single-parameter Hammett equation fails in many cases because the substituent constant, σ, is a combined measure of inductive and resonance effects. Since the relative contributions from each vary from system to system, researchers have advocated the use of modified substituent constants to account for such factors.[38] We have used a Hammett equation in which the substituent constant, σ, has been decomposed into its inductive and resonance components,

$$\sigma = \rho_I\sigma_I + \rho_R\sigma°_R$$

such that σ_I and $\sigma°_R$ are the inductive and resonance constants, respectively, and ρ_I and ρ_R are their corresponding weighting factors.[39] Both σ scales have been shown to be applicable to a wide selection of reactions with statistical reliability.[40]

The reduction potentials measured for **2**, **3**, **18**, and **19**, when fitted to this equation, give a very good correlation ($R^2 = 0.99$, $\rho_I = 0.49$, $\rho_R = 0.67$).[41] Figure 6 shows the linear correlation in the Hammett plot of the reduction potentials versus the modified substituent constants. The carbonyl stretching frequencies from both sets of dicarbonyl compounds were analyzed

(36) (a) Wells, P. R. *Linear Free Energy Relationships*; Academic Press: New York, 1968. (b) Johnson, C. D. *The Hammett Equation*; Cambridge University Press: London, 1973. (c) Lowry, T. H.; Richardson, K. S. *Mechanism and Theory in Organic Chemistry*; Harper & Row: New York, 1978. (d) Carpenter, B. K. *Determination of Organic Reaction Mechanisms*; John Wiley & Sons: 1984.

(37) Slocum, D. W.; Ernst, C. R. *Adv. Organomet. Chem.* **1972**, 10, 79.

(38) More than 20 different sets of substituent constants have been contrived, each representing a different blend of inductive and substituent contributions. See: Swain, C. G.; Lupton, E. C., Jr. *J. Am. Chem. Soc.* **1968**, 90, 4328 and references therein.

(39) Topsom, R. D. *Prog. Phys. Org. Chem.* **1976**, 12, 1.

(40) Ehrenson, S.; Brownlee, R. T. C.; Taft, R. W. *Prog. Phys. Org. Chem.* **1973**, 10, 1.

(41) Values for σ_I and $\sigma°_R$ were obtained from the following: (a) Hansch, C.; Leo, A. *Substituent Constants for Correlation Analysis in Chemistry and Biology*; John Wiley & Sons: New York, 1979. (b) Reference 35c. For R = NMe$_2$, OEt, Me, Ph, $\sigma_I = 0.06, 0.27, -0.04, 0.10$ and $\sigma°_R = -0.52, -0.45, -0.11, -0.11$, respectively.

Figure 7. Hammett plots of carbonyl stretching frequency for complexes **10**−**13** and **14**−**17** vs $\rho_I\sigma_I + \rho_R\sigma^\circ_R$.

accordingly, and these data are correlated linearly as well (Figure 7). The data from the dicarbonyl compounds $(C_5H_5B-R)_2Zr-(CO)_2$ (**14**−**17**) give rise to a better fit ($R^2 = 0.99$, $\rho_I = 46.5$, $\rho_R = 27.5$) than those of the mixed-ring dicarbonyls, **10**−**13** ($R^2 = 0.95$, $\rho_I = 27.2$, $\rho_R = 22.8$).

A similar Hammett analysis fails for the rate data listed in Table 2. There are two plausible reasons for this. First, the data set is small. Given that the exchange rates for **7** and **8** are nearly identical (Figure 4), extraction of the two ρ parameters is not possible. Second, we note that rate constants represent a more complicated probe for the evaluation of substituent effects in this type of analysis. Rate constants for a reaction system embody contributions from substituent effects, solvation energies, and very importantly, steric effects. Steric interactions between the exocyclic substituents and the borate anion are likely to be significant when the ion pair is tightly bound. Physical measurements are less subject to the aforementioned reaction variables and, therefore, may provide a more direct means for evaluating substituent effects.

Summary and Conclusion

In summary, the first well-defined ethylene polymerization catalysts supported by boratacyclic ligands have been synthesized and fully characterized. While the "typical" boratabenzene distortions are retained in **7** and **9**, differences in the cation−anion separation, which would indicate differences in ion-pairing strength, are not observed. We have shown that the role of the exocyclic boron substituent in tuning the electron density is an inherent feature in this class of catalysts by characterizing the impact of substitution on the kinetic profile of a catalytically significant elementary step. Ion-pair separation is facilitated by the presence of π-electrons on the boron substituent. That **6** and **7·**THF form from the reaction of **9** and **4** and also the reaction of **6** and **7** implies that the aminoboratabenzene ligand more effectively stabilizes a positive charge on zirconium.

The electrochemical and IR spectroscopic studies provide evidence for decreasing electron density at zirconium as a function of the exocyclic substituent of $[C_5H_5B-R]$ ligands in the order R = NMe_2 > OEt $\approx$ Me > Ph. Significantly, the data show satisfactory correlations with Hammett substituent constants σ_I and σ°_R. The relative contributions of ρ_I and ρ_R as a function of R depends on the nature of the experimental probe.

The Zr−CO stretching frequencies are apparently more sensitive to inductive perturbation from the exocyclic boron substituent; hence $[C_5H_5B-Me]$ is a stronger donor than $[C_5H_5B-OEt]$. Resonance effects contribute more strongly to the reduction potentials, and under this experimental probe, $[C_5H_5B-OEt]$ is a stronger donor than $[C_5H_5B-Me]$. As in the organic chemistry of aryl compounds, the nature of substituent effects depends on the mechanism of electron donation and the demands of the process under study.

Having collected rate information for an elementary reaction step and evaluated measures of electronic density at the metal center as a function of boratabenzene ligand, we find that making a direct correlation between the two data sets is not possible in all cases. For the extreme examples, R = NMe_2 and Ph, the clearly more donating aminoboratabenzene ligand is capable of affecting the reaction surface for the exchange reaction in a rational manner, i.e., by better stabilizing the more positively charged metal. Understanding the behavior of R = OEt, relative to R = NMe_2 and Ph, requires consideration of additional variables, such as steric effects.

In our efforts to quantify substituent effects, the solution dynamics studies provide the most persuasive evidence that simple substituent changes offer a direct means of tuning the activity and selectivity of boratabenzene catalysts. Most relevant is that our studies involve stoichiometrically precise, zwitterionic compounds. The reactions which use MAO are also likely to involve cationic species; however, MAO is a more complex and less defined coactivator than $B(C_6F_5)_3$. The observation that $AlMe_3$ forms an adduct with $(C_5H_5B-OEt)Cp*ZrCl_2$ via the oxygen atom is significant in this context since commercially available MAO may contain up to 35% of $AlMe_3$ by weight.[42] Thus, adducts of this type may play a role in determining product selectivity observed for **1**−**3**. The simplicity of structure makes $[(C_5H_5B-R)Cp*ZrMe][MeB(C_6F_5)_3]$ complexes such as **7**−**9** better candidates for a more precise and rational catalyst design.

Experimental Section

General Methods. All manipulations were performed under an inert atmosphere using standard glovebox and Schlenk techniques.[43] Solvents were degassed and distilled from the appropriate drying agents (EtO_2, THF, C_6H_6, toluene, and pentane from sodium−benzophenone). Deuterated solvents obtained from Cambridge Isotope Laboratories (all ≥99 atom % D) were treated similarly. $Cp*ZrCl_3$,[44] $Cp*ZrMe_2Cl$,[45] Li-$[C_5H_5B-NMe_2]$,[7g] $Na[C_5H_5B-OEt]$,[7g] $Li[C_5H_5B-Ph]$,[7b] and **19**[46] were prepared according to literature procedures. $B(C_6F_5)_3$ was received as a gift from Exxon Chemicals and was sublimed prior to use. Mg turnings (Aldrich) were stirred under vacuum prior to use. Ultrahigh-purity-grade (>99.99%) CO was purchased from Liquid Air Corp. ^1H NMR (400 MHz), ^{13}C NMR (400 MHz), and ^{11}B NMR spectra (128 MHz) were recorded on a Bruker AMX-400 spectrometer, while ^{19}F NMR (470 MHz) spectra were recorded on a Varian INOVA-500 spectrometer. Chemical shifts for ^1H NMR and ^{13}C NMR were referenced to internal solvent resonances. Those for ^{11}B NMR and ^{19}F NMR were referenced to external BF_3·OEt_2 and $CFCl_3$, respectively. Unless otherwise stated, all NMR spectra were recorded at room temperature. Infrared data were recorded on a Mattson Instruments

(42) Rogers, J. S.; Lachicotte, R. J.; Bazan, G. C. *J. Am. Chem. Soc.* **1999**, *121*, 1288.

(43) Burger, B. J.; Bercaw, J. E. In *Experimental Organometallic Chemistry*; Wayda, A. L., Darensbourg, M. Y., Eds.; ACS Symposium Series 357; American Chemical Society: Washington, DC, 1987.

(44) Wolczanski, P. T.; Bercaw, J. E. *Organometallics* **1982**, *1*, 793.

(45) Rodriguez, G. Ph.D. Thesis, University of Rochester, 1997.

(46) Herberich, G. E.; Englert, U.; Schmitz, A. *Organometallics* **1997**, *16*, 3751.

(47) Sikora, D. J.; Macomber, D. W.; Rausch, M. D. *Adv. Organomet. Chem.* **1986**, *25*, 317.

Genesis series FT-IR spectrometer. The Nujol used for the analyses was dried over sodium dispersion, degassed, and filtered prior to use. IR spectra were referenced internally to the CH_2 rocking band at 723.1 cm^{-1}. Elemental analyses were performed by Desert Analytics, Tuscon, AZ.

($C_5H_5B-NMe_2$)Cp*ZrMe$_2$ (4). A solution containing 50.0 mg (0.394 mmol) of Li[$C_5H_5B-NMe_2$] in 5 mL of Et$_2$O was added to 115.0 mg (0.394 mmol) of Cp*ZrMe$_2$Cl in 10 mL of Et$_2$O at −35 °C. After 2 h of stirring, the solution was filtered, and the solvent was removed in vacuo. Recrystallization of crude product from pentane at −35 °C afforded yellow flakes (122 mg, 82%). ^{1}H NMR (C_6D_6): δ 6.51 (dd, 2H, $J = 10.9, 6.6$ Hz, H$_β$), 5.58 (dd, 2H, $J = 10.8, 1.2$ Hz, H$_α$), 5.13 (tt, 1H, $J = 6.6, 1.2$ Hz, H$_γ$), 2.81 (s, 6H, NCH_3), 1.69 (s, 15H, C$_5$-(CH_3)$_5$), −0.22 (s, 6H, ZrCH_3). ^{13}C{^{1}H} NMR (C_6D_6): δ 137.1 (C$_β$), 118.2 (C$_5$(CH$_3$)$_5$), 114.8 (br, C$_α$), 97.7 (C$_γ$), 38.4 (ZrCH$_3$), 34.7 (NCH$_3$), 11.7 (C$_5$(CH$_3$)$_5$). ^{11}B{^{1}H} NMR: δ 32.0. Anal. Calcd (C$_{19}$H$_{32}$-BNZr): C, 60.61; H, 8.57; N, 3.72. Found: C, 60.36; H, 8.39; N, 3.48.

(C_5H_5B-OEt)Cp*ZrMe$_2$ (5). A solution containing 90.0 mg (0.625 mmol) of [C_5H_5B-OEt]Na in 5 mL of THF was added to 182.5 mg (0.625 mmol) of Cp*ZrMe$_2$Cl in 10 mL of Et$_2$O at −35 °C. The reaction mixture was stirred overnight. Evaporation of the solvent gave a yellow solid. The product was extracted into pentane, and the extract was filtered and reduced in volume. Recrystallization from pentane at −35 °C gave clear, pale yellow plates (212 mg, 90%). ^{1}H NMR (C_6D_6): δ 6.58 (dd, 2H, $J = 10.9, 6.7$ Hz, H$_β$), 5.70 (dd, 2H, $J = 11.0, 1.4$ Hz, H$_α$), 5.25 (tt, 1H, $J = 6.7, 1.4$ Hz, H$_γ$), 4.06 (q, 2H, $J = 7.0$ Hz, OCH_2), 1.64 (s, 15H, C$_5$(CH_3)$_5$), 1.37 (t, 3H, $J = 7.0$ Hz, OCH$_2$CH_3), −0.17 (s, 6H, ZrCH_3). ^{13}C{^{1}H} NMR (C_6D_6): δ 138.6 (C$_β$), 118.6 (C$_5$(CH$_3$)$_5$), 116.1 (br, C$_α$), 100.9 (C$_γ$), 60.5 (OCH$_2$), 38.9 (ZrCH$_3$), 17.8 (OCH$_2$CH$_3$), 11.6 (C$_5$(CH$_3$)$_5$). ^{11}B{^{1}H} NMR (C_6D_6): δ 35.9. Anal. Calcd (C$_{19}$H$_{31}$-BOZr): C, 60.45; H, 8.28. Found: C, 60.56; H, 8.19.

(C_5H_5B-Ph)Cp*ZrMe$_2$ (6). A solution containing 50.0 mg (0.313 mmol) of [C_5H_5B-Ph]Li in 5 mL of Et$_2$O was added to 91.0 mg (0.312 mmol) of Cp*ZrMe$_2$Cl in 10 mL of Et$_2$O at −35 °C. After 4 h of stirring, the reaction mixture was filtered, and the solvent was removed in vacuo to afford a tan solid. The crude product was extracted into pentane, and the extract was filtered. The solution was reduced in volume, and upon standing overnight at −35 °C, tan crystals deposited. Recrystallization in the same manner afforded a second crop (116 mg, 91%). ^{1}H NMR (C_6D_6): δ 8.05 (d, 2H, $J = 6.8$ Hz, o-H), 7.43 (t, 2H, $J = 7.5$ Hz, m-H), 7.30 (tt, 1H, $J = 7.3, 1.2$ Hz, p-H), 6.77 (m, 4H, H$_α$ and H$_β$), 5.73 (tt, 1H, $J = 6.2, 2.1$ Hz, H$_γ$), 1.58 (s, 15H, C$_5$(CH_3)$_5$), −0.29 (s, 6H, ZrCH_3). ^{13}C{^{1}H} NMR (C_6D_6): δ 136.7 (C$_β$), 133.4 (o-C), 128.6 (p-C), 128.1 (m-C), 118.8 (C$_5$(CH$_3$)$_5$), 108.6 (C$_γ$), 38.8 (ZrCH$_3$), 11.6 (C$_5$(CH$_3$)$_5$), C$_α$ not observed. ^{11}B{^{1}H} NMR (C_6D_6): δ 37.3. Anal. Calcd (C$_{23}$H$_{31}$BZr): C, 67.46; H, 7.63. Found: C, 66.15; H, 7.48.

[($C_5H_5B-NMe_2$)Cp*ZrMe][MeB(C_6F_5)$_3$] (7). A solution containing 50.0 mg (0.096 mmol) of B(C_6F_5)$_3$ in 5 mL of toluene was added to a stirred solution containing 36.7 mg (0.096 mmol) of **4** in 3 mL of toluene at −35 °C. The biphasic solution became homogeneous gradually upon warming and darkened to a crimson color. Approximately 10 mL of pentane was added to the solution with rapid stirring. Slow recrystallization at −35 °C afforded dark red plates (80 mg, 92%). ^{1}H NMR (228 K, toluene-d_8): δ 6.37 (dd, 1H, $J = 10.0, 7.8$ Hz, H$_β'$), 5.72 (dd, 1H, $J = 10.8, 6.9$ Hz, H$_β$), 5.33 (d, 1H, $J = 9.2$ Hz, H$_α'$), 5.08 (t, 1H, $J = 6.8$ Hz, H$_γ$), 4.45 (d, 1H, $J = 10.7$ Hz, H$_α$), 2.61 (s, 3H, NCH_3'), 2.31 (s, 3H, NCH_3), 1.24 (s, 15H, C$_5$(CH_3)$_5$), 0.50 (s, 3H, ZrCH_3), −0.19 (br s, 3H, BCH_3). ^{13}C{^{1}H} NMR: δ 148.8 (d, $^1J_{C-F} = 230.9$ Hz), 139.5 (C$_β$), 139.4 (d, $^1J_{C-F} = 249.4$ Hz), 137.5 (d, $^1J_{C-F} = 248.5$ Hz), 116.0 (br, C$_α$). 99.1 (C$_γ$), 44.1 (ZrCH$_3$), 37.7 (NCH$_3$), 11.5 (C$_5$(CH$_3$)$_5$), C$_5$(CH$_3$)$_5$ and BCH$_3$ not observed. ^{11}B{^{1}H} NMR (toluene-d_8): δ −8.5 (BCH$_3$), C$_5H_5$B not observed. ^{19}F NMR (toluene-d_8): δ −134.0 (s, o-F), −160.9 (s, p-F), −165.7 (s, m-F). Anal. Calcd (C$_{37}$H$_{32}$B$_2$F$_{15}$NZr·C$_7$H$_8$): C, 53.89; H, 4.11; N, 1.43. Found: C, 53.00; H, 3.98; N, 1.19.

[(C_5H_5B-OEt)Cp*ZrMe][MeB(C_6F_5)$_3$] (8). A solution containing 33.8 mg (0.066 mmol) of B(C_6F_5)$_3$ in 5 mL of toluene was added to a stirred solution containing 24.6 mg (0.065 mmol) of **5** in 5 mL of toluene at −35 °C. The biphasic, light yellow solution gradually became homogeneous upon prolonged stirring. A 10 mL aliquot of pentane

was added to the solution with rapid stirring. The prolonged storage of this solution at −35 °C gave an amorphous yellow solid (47 mg, 81%). ^{1}H NMR (243 K, toluene-d_8): δ 6.66 (dd, 1H, $J = 10.7, 5.7$ Hz, H$_β'$), 6.56 (br t, 1H, $J = 8.4$ Hz, H$_β$), 6.45 (d, 1H, $J = 10.2$ Hz, H$_α'$), 5.51 (d, 1H, $J = 9.6$ Hz, H$_α$), 5.37 (t, 1H, $J = 6.8$ Hz, H$_γ$), 3.98 (m, 2H, $J = 6.8$ Hz, OCH_2). 1.24 (s, 15H, C$_5$(CH_3)$_5$), 1.05 (t, 3H, $J = 6.8$ Hz, OCH$_2$CH_3), 0.68 (s, 3H, ZrCH_3), 0.34 (br s, 3H, BCH_3). ^{13}C{^{1}H} NMR (toluene-d_8): δ 149.0 (d, $^1J_{C-F} = 240.1$ Hz), 142.8 (C$_β$), 139.0 (d, $^1J_{C-F} = 247.7$ Hz), 137.6 (d, $^1J_{C-F} = 246.0$ Hz), 127.0 (C$_5$(CH$_3$)$_5$), 107.6 (C$_γ$), 73.2 (OCH$_2$), 49.5 (ZrCH$_3$), 18.4 (OCH$_2$CH$_3$), 11.4 (C$_5$CH$_3$)$_5$), C$_α$ and BCH$_3$ not observed. ^{11}B{^{1}H} NMR (toluene-d_8): δ −0.85 (BCH$_3$), C$_5H_5$B not observed. ^{19}F NMR (toluene-d_8): δ −133.6 (s, o-F), −160.8 (s, p-F), −165.6 (s, m-F). Anal. Calcd (C$_{37}$H$_{31}$B$_2$F$_{15}$OZr): C, 49.96; H, 3.51. Found: C, 49.93; H, 3.55.

[(C_5H_5B-Ph)Cp*ZrMe][MeB(C_6F_5)$_3$] (9). A solution containing 50.0 mg (0.096 mmol) of B(C_6F_5)$_3$ in 5 mL of toluene was cooled to −35 °C. This solution was slowly added to a stirred solution containing 40.0 mg (0.096 mmol) of **6** in 5 mL of toluene at −35 °C. The pale yellow solution became homogeneous gradually upon warming and turned bright yellow. The solution was reduced in volume, and pentane was added with stirring until incipient precipitation was observed. Once the solution regained homogeneity, it was stored at −35 °C, whereupon yellow crystals deposited (74 mg, 82). ^{1}H NMR (258 K, toluene-d_8): δ 7.76 (d, 2H, $J = 6.9$ Hz, o-H), 7.34 (t, 2H, $J = 7.3$ Hz, m-H), 7.26 (t, 1H, $J = 7.3$ Hz, p-H), 7.04 (d, 1H, $J = 9.3$ Hz, H$_α'$), 6.72 (dd, 1H, $J = 10.8, 6.7$ Hz, H$_β'$), 5.95 (br t, 1H, $J = 8.4$ Hz, H$_β$), 5.59 (t, 1H, $J = 6.7$ Hz, H$_γ$), 5.45 (d, 1H, $J = 10.4$ Hz, H$_α$), 1.18 (s, 15H, C$_5$(CH_3)$_5$), 0.44 (s, 3H, ZrCH_3), −0.34 (br s, 3H, BCH_3). ^{13}C{^{1}H} NMR (toluene-d_8): δ 148.8 (d, $^1J_{C-F} = 236.8$ Hz), 139.5 (d, $^1J_{C-F} = 244.7$ Hz), 139.2 (C$_β$), 137.6 (d, $^1J_{C-F} = 248.2$ Hz), 133.2 (o-C), 130.4 (p-C), 128.6 (m-C), 126.2 (C$_5$(CH$_3$)$_5$), 123.6 (br, C$_α$), 108.1 (C$_γ$), 52.4 (ZrCH$_3$), 24.1 (br, BCH$_3$), 11.6 (C$_5$(CH$_3$)$_5$). ^{11}B{^{1}H} NMR (toluene-d_8): δ −8.5 (BCH$_3$), C$_5H_5$B not observed. ^{19}F NMR (toluene-d_8): δ −134.3 (s, o-F), −160 (t, $^3J_{F-F} = 19.4$ Hz, p-F), −165.2 (s, m-F). Anal. Calcd (C$_{41}$H$_{31}$B$_2$F$_{15}$Zr): C, 53.44; H, 3.39. Found: C, 53.42; H, 3.57.

Observation of [(C_5H_5B-Me)Cp*ZrMe][MeB(C_6F_5)$_3$]. A solution containing 33.8 mg (0.066 mmol) of B(C_6F_5)$_3$ in 5 mL of toluene was added to a stirred solution containing 22.6 mg (0.065 mmol) of (C_5H_5B-Me)Cp*ZrMe$_2$ in 5 mL of toluene at −35 °C. ^{1}H NMR (243 K, toluene-d_8): δ 6.52 (dd, 1H, $J = 10.5, 7.0$ Hz, H$_β'$), 6.43 (d, 1H, $J = 11.0$ Hz, H$_α'$), 5.85 (dd, 1H, $J = 10.0, 7.5$ Hz, H$_β$), 5.45 (t, 1H, $J = 7.0$ Hz, H$_γ$), 4.84 (d, 1H, $J = 10.0$ Hz, H$_α$), 1.19 (s, 15H, C$_5$(CH_3)$_5$), 0.82 (s, 3H, C$_5H_5$B−CH_3), 0.55 (s, 3H, ZrCH_3), −0.37 (br, 3H, (C$_6F_5$)$_3$-BCH_3). ^{13}C{^{1}H} NMR (toluene-d_8): δ 148.8 (d, $J_{C-F} = 237.0$ Hz), 139.8 (d, $J_{C-F} = 193.0$ Hz), 139.2 (C$_β$), 134.9 (d, $J_{C-F} = 282.2$ Hz), 125.9 (C$_5$(CH$_3$)$_5$), 123.4 (br, C$_α$), 107.0 (C$_γ$), 49.6 (ZrCH$_3$), 24.8 (C$_5H_5$B−CH$_3$), 11.5 (C$_5$CH$_3$)$_5$), 6.0 ((C$_6F_5$)$_3$BCH$_3$). ^{11}B{^{1}H} NMR (toluene-d_8): δ 46.5 (br, C$_5H_5$B), −13.8 ((C$_6F_5$)$_3$BCH$_3$). ^{19}F NMR (toluene-d_8): δ −135.0 (s, o-F), −161.0 (s, p-F), −166.0 (s, m-F).

THF-d_8 Adducts of 5−8. The adducts were prepared in situ by the dropwise addition of THF-d_8 to stirred solutions of **5−8** in toluene-d_8. Phase separation occurred initially, and the reaction mixture remained heterogeneous until a sufficient amount of THF-d_8 was added. The amount of THF-d_8 required for complete dissolution varied for each compound.

[($C_5H_5B-NMe_2$)Cp*ZrMe(THF-d_8)][MeB(C_6F_5)$_3$]. ^{1}H NMR (toluene-d_8/THF-d_8): δ 7.11 (ddd, 1H, $J = 11.6, 6.4, 2.0$ Hz, H$_β'$), 6.88 (ddd, 1H, $J = 11.2, 6.8, 2.0$ Hz, H$_β$), 6.26 (ddd, 1H, $J = 11.6, 3.2, 1.6$ Hz, H$_α'$), 5.95 (tt, 1H, $J = 6.4, 1.6$ Hz, H$_γ$), 5.36 (ddd, 1H, $J = 11.2, 3.2, 1.6$ Hz H$_α$), 2.88 (s, 3H, NCH_3'), 2.74 (s, 3H, NCH_3), 2.02 (s, 15H, C$_5$(CH_3)$_5$), 0.56 (s, 3H, ZrCH_3), 0.51 (br, 3H, BCH_3).

[(C_5H_5B-OEt)Cp*ZrMe(THF-d_8)][MeB(C_6F_5)$_3$]. ^{1}H NMR (toluene-d_8/THF-d_8): δ 7.09 (ddd, 1H, $J = 10.0, 7.4, 1.6$ Hz H$_β'$), 6.95 (ddd, 1H, $J = 11.2, 6.8, 1.6$ Hz, H$_β$), 6.57 (ddd, 1H, $J = 11.2, 2.4, 1.6$ Hz, H$_α'$), 6.15 (ddd, 1H, $J = 10.4. 2.8, 1.6$ Hz, H$_α$), 5.80 (tt, 1H, $J = 6.8, 1.6$ Hz H$_γ$), 4.00 (dq, 1H, $J = 11.4, 6.8$ Hz, OCH'), 3.88 (dq, 1H, $J = 11.4, 6.8$ Hz, OCH), 1.58 (s, 15H, C$_5$(CH_3)$_5$), 1.11 (br, 3H, BCH_3), 0.95 (t, 3H, $J = 6.8$ Hz, OCH$_2$CH_3), 0.61 (s, 3H, ZrCH_3).

[(C_5H_5B-Ph)Cp*ZrMe(THF-d_8)][MeB(C_6F_5)$_3$]. ^{1}H NMR (toluene-d_8/THF-d_8): δ 7.76 (d, 2H, $J = 6.9$ Hz o-H), 7.34 (t, 2H, $J = 17.3$ Hz, m-H), 7.26 (t, 1H, $J = 7.3$ Hz, p-H), 6.92 (ddd, 1H, $J = 10.8, 2.8, 1.6$

Hz, H$_\alpha'$), 6.87 (ddd, 1H, J = 10.6. 7.2, 1.6 Hz, H$_\beta'$), 6.79 (ddd, 1H, J = 10.8, 6.8, 1.6 Hz, H$_\beta$), 6.37 (ddd, 1H, J = 10.6, 2.8, 1.6 Hz, H$_\alpha$), 5.84 (tt, 1H, J = 6.8, 1.6 Hz, H$_\gamma$), 1.48 (s, 15H, C$_5$(CH$_3$)$_5$), 1.11 (br, 3H, BCH$_3$), 0.27 (s, 3H, ZrCH$_3$).

[(C$_5$H$_5$B−Me)Cp*ZrMe(THF-d_8)][MeB(C$_6$F$_5$)$_3$]. ^{1}H NMR (toluene-d_8/THF-d_8): δ 6.68 (ddd, 1H, J = 10.8, 6.8, 2.0 Hz, H$_\beta'$), 6.47 (ddd, 1H, J = 10.8, 6.8, 2.0 Hz, H$_\beta$), 6.46 (ddd, 1H, J = 10.4, 2.8, 1.6 Hz, H$_\alpha'$), 6.00 (tt, 1H, J = 6.8, 1.6 Hz, H$_\gamma$), 5.30 (ddd, 1H, J = 10.4, 2.8, 1.6 Hz, H$_\alpha$), 1.50 (s, 15H, C$_5$(CH$_3$)$_5$), 1.08 (br, 3H, BCH$_3$), 0.78 (s, 3H, C$_5$H$_5$B−CH$_3$), 0.31 (s, 3H, ZrCH$_3$).

(C$_5$H$_5$B−R)Cp*Zr(CO)$_2$ (R = NMe$_2$ (10), OEt (11), Me (12) Ph (13)). The following procedure is representative. A solution containing 50 mg of (C$_5$H$_5$B−R)Cp*ZrCl$_2$ in 5 mL of THF was placed into a Schlenk bomb. Two crushed magnesium turnings (approximately 5 mg) were added to the solution. The reaction vessel was attached to the high-vacuum line. After the bomb was partially evacuated, 700 Torr of CO was introduced over the solution. The reaction mixture was stirred for 2−3 h, whereupon the solution turned dark red. The volatiles were removed in vacuo, and the residue was extracted with benzene. The extract was filtered, and the solvent was removed to give a dark red oil. The crude material was extracted into heptane or pentane, and the extract was filtered. Removal of the solvent afforded a dark red oil or a red solid.

10. After prolonged exposure to high vacuum, the oil solidified into an amorphous solid (20 mg, 40%). ^{1}H NMR (C$_6$D$_6$): δ 5.59 (dd, 2H, J = 10.1, 6.9 Hz, H$_\beta$), 4.58 (tt, 1H, J = 6.8, 1.4 Hz, H$_\gamma$), 4.10 (dd, 2H, J = 10.0, 1.3 Hz, H$_\alpha$), 2.54 (s, 6H, NCH$_3$), 1.69 (s, 15H, C$_5$(CH$_3$)$_5$). ^{13}C{^{1}H} NMR (C$_6$D$_6$): δ 249.6 (CO), 115.2 (C$_5$(CH$_3$)$_5$), 107.0 (C$_\beta$), 96.0 (C$_\gamma$), 84.6 (br, C$_\alpha$), 38.1 (NCH$_3$), 11.4 (C$_5$(CH$_3$)$_5$. ^{11}B{^{1}H} NMR (C$_6$D$_6$): δ 25.8. IR ν(CO): 1976, 1908 cm^{-1}. Anal. Calcd (C$_{19}$H$_{26}$BNO$_2$Zr): C, 56.70; H, 6.51; N, 3.48. Found: C, 56.44; H, 6.23; N, 2.86.

11. Crude crystals formed in the oil upon standing. The product was recrystallized from pentane at −35 °C as dark red granules (23 mg, 48%). ^{1}H NMR (C$_6$D$_6$): δ 5.59 (dd, 2H, J = 10.1, 7.0 Hz, H$_\beta$), 4.61 (tt, 1H, J = 6.9, 1.5 Hz, H$_\gamma$), 4.33 (dd, 2H, J = 9.9, 1.4 Hz, H$_\alpha$), 3.75 (q, 2H, J = 7.0 Hz, OCH$_2$), 1.63 (s, 15H, C$_5$(CH$_3$)$_5$), 1.24 (t, 3H, J = 7.0 Hz, OCH$_2$CH$_3$). ^{13}C{^{1}H} NMR (C$_6$D$_6$): δ 250.5 (CO), 116.3 (C$_5$(CH$_3$)$_5$), 107.0 (C$_\beta$), 98.0 (C$_\gamma$), 88.5 (br C$_\alpha$), 60.4 (OCH$_2$), 17.4 (OCH$_2$CH$_3$), 11.3 (C$_5$(CH$_3$)$_5$). ^{11}B{^{1}H} NMR (C$_6$D$_6$): δ 30.1. IR ν(CO): 1982, 1914 cm^{-1}. Anal. Calcd (C$_{19}$H$_{25}$BO$_3$Zr): C, 56.57; H, 6.25. Found: C, 56.64; H, 6.44.

12. ^{1}H NMR (C$_6$D$_6$): δ 5.57 (dd, 2H, J = 9.6, 7.2 Hz, H$_\beta$), 4.84 (tt, 1H, J = 7.2, 1.6 Hz, H$_\gamma$), 4.75 (dd, 2H, J = 9.6, 1.6 Hz, H$_\alpha$), 1.61 (s, 15H, C$_5$(CH$_3$)$_5$), 0.74 (s, 3H, BCH$_3$). ^{13}C{^{1}H} NMR (C$_6$D$_6$): δ 252.9 (CO), 116.3 (C$_5$(CH$_3$)$_5$), 106.7 (C$_\beta$), 102.6 (br C$_\alpha$), 101.4 (C$_\gamma$), 11.3 (C$_5$(CH$_3$)$_5$). ^{11}B{^{1}H} NMR (C$_6$D$_6$): δ 32.8. IR ν(CO): 1981, 1913 cm^{-1}.

13. ^{1}H NMR (C$_6$D$_6$): δ 7.85 (d, 2H, J = 8.2 Hz, o-H), 7.34 (t, 2H, J = 7.6 Hz, m-H), 7.25 (t, 1H, J = 7.6 Hz, p-H), 5.65 (dd, 2H, J = 9.6, 6.8 Hz, H$_\beta$), 5.19 (dd, 2H, J = 9.6, 1.6 Hz, H$_\alpha$), 4.92 (tt, 1H, J =

6.8, 1.6 Hz, H$_\gamma$), 1.57 (s, 15H, C$_5$(CH$_3$)$_5$). ^{13}C{^{1}H} NMR (C$_6$D$_6$): δ 251.0 (CO), 132.9 (o-C), 128.5 (p-C), 127.9 (m-C), 116.4 (C$_5$(CH$_3$)$_5$), 107.0 (C$_\beta$), 102.4 (C$_\gamma$), 100.2 (br, C$_\alpha$), 11.3 (C$_5$(CH$_3$)$_5$. ^{11}B{^{1}H} NMR (C$_6$D$_6$): δ 30.1. IR ν(CO): 1987, 1920 cm^{-1}.

(C$_5$H$_5$B−R)$_2$Zr(CO)$_2$ (R = NMe$_2$ (14), OEt (15), Me (16), Ph (17)). The general procedure described above was followed using (C$_5$H$_5$B−R)$_2$ZrCl$_2$ as the starting materials.

14. The product was recrystallized from pentane at −35 °C as dark red fibers (37 mg, 78%). ^{1}H NMR (C$_6$D$_6$): δ 5.70 (dd, 4H, J = 10.4, 6.8 Hz, H$_\beta$), 4.53 (tt, 2H, J = 6.8, 1.6 Hz, H$_\gamma$), 4.10 (dd, 4H, J = 10.0, 1.6 Hz, H$_\alpha$), 2.56 (s, 12H, NCH$_3$). ^{13}C {^{1}H} NMR (C$_6$D$_6$): δ 232.8 (CO), 113.0 (C$_\beta$), 91.4 (C$_\gamma$), 83.9 (br, C$_\alpha$), 37.9 (NCH$_3$). ^{11}B{^{1}H} NMR (C$_6$D$_6$): δ 26.2. IR ν(CO): 2005, 1955 cm^{-1}. Anal. Calcd (C$_{16}$H$_{22}$B$_2$N$_2$O$_2$Zr): C, 49.63; H, 5.73; N, 7.23. Found: C, 49.10; H, 6.06; N, 6.17.

15. ^{1}H NMR (C$_6$D$_6$): δ 5.65 (dd, 4H, J = 10.4, 6.8 Hz, H$_\beta$), 4.50 (tt, 2H, J = 6.8, 1.6 Hz, H$_\gamma$), 4.29 (dd, 4H, J = 10.4, 1.6 Hz, H$_\alpha$), 3.73 (q, 4H, J = 7.2 Hz, OCH$_2$), 1.23 (t, 6H, J = 7.2 Hz, OCH$_2$CH$_3$). ^{13}C{^{1}H} NMR (C$_6$D$_6$): δ 234.0 (CO), 114.0 (C$_\beta$), 93.3 (C$_\gamma$), 87.8 (br C$_\alpha$), 60.5 (OCH$_2$), 17.4 (OCH$_2$CH$_3$). ^{11}B{^{1}H} NMR (C$_6$D$_6$): δ 30.1. IR ν(CO): 2017, 1969 cm^{-1}.

16. ^{1}H NMR (C$_6$D$_6$): δ 5.60 (dd, 4H, J = 10.0, 6.8 Hz, H$_\beta$), 4.67 (tt, 2H, J = 6.8, 1.6 Hz, H$_\gamma$), 4.65 (dd, 4H, J = 10.0, 1.6 Hz, H$_\alpha$), 0.74 (s, 6H, BCH$_3$). ^{13}C{^{1}H} NMR (C$_6$D$_6$): δ 237.2 (CO), 113.6 (C$_\beta$), 101.6 (br C$_\alpha$), 96.4 (C$_\gamma$), 4.6 (br, BCH$_3$). ^{11}B{^{1}H} NMR (C$_6$D$_6$): δ 33.2. IR ν(CO): 2012, 1964 cm^{-1}.

17. The residue was extracted into hot heptane, and the extract was filtered. Slow cooling resulted in the precipitation of a dark red powder (16 mg, 31%). ^{1}H NMR (C$_6$D$_6$): δ 7.77 (dd, 4H, J = 8.1, 1.4 Hz, o-H), 7.33 (t, 4H, J = 7.1 Hz, m-H), 7.26 (tt, 2H, J = 7.2, 1.2 Hz, p-H), 5.71 (dd, 4H, J = 9.9, 7.0 Hz, H$_\beta$), 5.12 (dd, 4H, J = 9.9, 1.6 Hz, H$_\alpha$), 4.77 (tt, 2H, J = 7.0, 1.6 Hz, H$_\gamma$). ^{13}C{^{1}H} NMR (C$_6$D$_6$): δ 235.0 (CO), 133.5 (o-C), 132.7 (p-C), 130.3 (m-C), 114.1 (C$_\beta$), 99.7 (br C$_\alpha$), 99.2 (C$_\gamma$). ^{11}B{^{1}H} NMR (C$_6$D$_6$): δ 30.4. IR ν(CO): 2018, 1965 cm^{-1}. Anal. Calcd (C$_{24}$H$_{20}$B$_2$O$_2$Zr): C, 63.60; H, 4.45. Found: C, 62.63; H, 3.56.

Supporting Information Available: Complete X-ray crystallographic data for complexes **7** and **9** (PDF). See also Table 5. This material is available free of charge via the Internet at http://pubs.acs.org.

JA992413+